Indian Journal of Pure & Applied Physics
Vol. 55, June 2017, pp. 413-419

Thermoluminescence studies of $CaSO_4$: Eu nanophosphor for electron dosimetry

Nandkumar Mandlik[a], V N Bhoraskar[b], B J Patil[c], S S Dahiwale[b], P D Sahare[d] & S D Dhole[b]*

[a]Department of Physics, Fergusson College, S P Pune University, Pune 411 004, India
[b]Department of Physics, S P Pune University, Pune 411 007, India
[c]Department of Physics, Abasaheb Garware College, S P Pune University, Pune 411 004, India
[d]Department of Physics and Astrophysics, University of Delhi, Delhi 110 007, India

Received 28 November 2014; revised 4 April 2017; accepted 19 April 2017

Sample of $CaSO_4$: Eu nanophosphor has been synthesized by chemical co-precipitation method and irradiated with 6.5 MeV electrons over the fluence range from 5×10^{14} to 4×10^{15} e/cm^2. The as-synthesized sample has been characterized by the XRD and TEM. The TEM image reveals that the nanocrystallites are in the form of nanorods of length 75 to 125 nm, with varying diameter of 10 to 20 nm. The XRD yields an average grain size ~15 nm, with hexagonal structure. The electron irradiated samples exhibit the thermoluminescence glow curve with a single peak at 162 °C. Moreover, the TL peak intensity increases with the increase in electron fluence and saturates beyond 3×10^{15} e/cm^2. Moreover, TL glow curves have been theoretically fitted using computerized glow curve deconvolution (CGCD) method to determine trapping parameters. The results indicate that $CaSO_4$: Eu can be used as a dosimeter for 6.5 MeV electrons over dose range from 15-80 kGy.

Keywords: Thermoluminescence, Nanophosphor, Deconvolution, Radiation dosimetry

1 Introduction

The physical, chemical, electrical and optical properties of nanocrystalline materials are size and shape dependent and they often exhibit important differences in the bulk properties. Nanophase materials can form new and metastable crystal structures and have potential as efficient phosphors. Recently, nanocrystalline materials have attracted many researchers due to their potential applications in many diverged fields[1,2]. Thermoluminescence (TL) is a very popular and simple technique used for radiation dosimetry. The intensity of light emitted by phosphor is proportional to the irradiation doses given to it and by calibration with known doses of high-energy radiations an unknown doses could also be estimated. Rare earth doped mixed sulphates systems have been found to be good TL phosphors, e.g., microcrystalline potassium calcium sulphate doped with europium, i.e., $K_2Ca_2(SO_4)_3$: Eu, is found to be very high sensitive phosphor[3]. Later researchers have studied many TLD phosphors in their nanocrystalline forms and found that nanocrystalline forms of such TLD phosphors have improved characteristics for their potential applications in dosimetry of ionizing radiations over a very wide range and especially, for high doses, where the commercially used microcrystalline phosphors fail due to saturation besides the method of preparation of these materials being very simple[4-7]. Generally, TL phosphors that have been used for dosimetry for ionizing radiations such as X-ray and gamma rays are in the microcrystalline forms. However, the study on TL behavior of nanocrystalline materials has shown that the nanophosphors have somewhat poor sensitivity particularly at low doses as compared with microcrystalline phosphors. But they exhibit an excellent linear response at high doses in contrast with the microcrystalline phosphors which generally saturates at high doses. This particular aspect makes them suitable for dosimetry at high doses[6-9]. Recently, reports on some nanophosphors such as $CaSO_4$:Dy, $K_2Ca_2(SO_4)_3$: Eu, LiF:Mg, Cu, P and $Ba_{0.97}Ca_{0.03}SO_4$: Eu show quite suitable for estimating very high doses (~100 kGy) for high-energy radiations like gamma rays, protons and heavy ions[6-10].

The charged particles such as electrons, ions and protons, etc., are the main source of radiation contributing to the dose in space and they generate a serious problem of damaging the components used in various subsystems of the space craft. It can be checked by manufacturing the radiation resistant materials which further estimates the dose in that

*Corresponding author (E-mail: sanjay@physics.unipune.ac.in)

particular area. This can be achieved by proper and systematic radiation dosimetry done by a reliable TLD material. Therefore, the TL technique requires small TLD chips or even powder which can simply be mounted and measure the dose[11]. In addition, high dose electron dosimetry is being used very often for radiation therapy and radiography. Since last many years glow curve deconvolution (GCD) programs have been developed and applied to analyze the nature of traps[4,7,8,12]. Deconvolution of TL glow curve is important, as many trapping parameters such as trap depth, order of kinetics, frequency factor, and maximum peak temperature can be calculated.

$CaSO_4$ doped with various rare earth materials have been extensively investigated by several researchers[2,13-17]. The key features are being high sensitivity and good performances for gamma dosimetry. But, there are not many reports on the thermoluminescence characteristic of nanophosphors with electron irradiation. Therefore, in the present study a $CaSO_4$: Eu nanophosphor has been prepared by co-precipitation method and especially, dosimetric view has been studied for high energy electrons. Further, the TL characteristic has been correlated with electron dose. In addition, TL glow curves are deconvoluted using computerized glow curve deconvolution (CGCD) method and various trapping parameters, such as, activation energy (E), order of kinetics (b) and frequency factors (s) have been determined. The aim of the present work is to investigate some of the thermoluminescent properties of $CaSO_4$: Eu irradiated with high energy electron beam for high dose measurement.

2 Experimental

2.1 Method of preparation

Nanorods of $CaSO_4$: Eu was prepared by the following reaction[1]:

$$(CH_3COO)_2Ca + (NH_4)_2SO_4 + EuCl_2(0.1\ \text{mol}\%) \xrightarrow{EtOH+\ {}_2O} CaSO_4{:}Eu \downarrow +2CH_3COONH_4 \quad \ldots (1)$$

The raw materials used for preparation of $CaSO_4$: Eu nanorods were $(CH_3COO)_2Ca$ 99% (HPLC), $(NH_4)_2SO_4$ 99.5% (Merck), $EuCl_2$ 99.99% (Aldrich), ethanol of AR grade and double distilled water. About 3.105 g of calcium acetate was dissolved in 100 mL double distilled water (0.5 N solution) and then 5.56 mg of $EuCl_2$ (0.1 mol%) was added to the respective solution. Further, 100 mL ethanol was also added in the above solution. Moreover, about 3.3 g of $(NH_4)_2SO_4$ was dissolved in 100 mL double distilled water (0.5 N solution) and the same solution was added to calcium acetate solution drop wise under vigorous stirring. White precipitate was formed which was then filtered and washed several times to remove the residual salts. Nanocrystalline powder samples thus obtained were dried at 150 °C in an oven for 12 h. This as synthesized powder sample was used for further characterization.

2.2 Characterization

To confirm the formation of the compound, X-ray diffraction pattern was studied at room temperature by using Cu-target (CuK_α = 1.54 Å) on Bruker AXS D8 Advance X-ray diffractometer and matched with the standard data available (JCPDS card No. 43-0606). Broadening in the X-ray diffraction peaks of the nanocrystalline powder was utilized to determine the particle size using Scherrer's formula. TEM image has been obtained on transmission electron microscope, TECHNAI G2 20U–TWIN (FEI, Netherlands), operated at 200 kV. For taking TEM images, 1 mg powder sample was put in 4 mL of ethanol and ultrasonicated for 10 min to form a suspension. A drop of this suspension was put on a carbon coated copper grid (200 mesh) and dried in air for half an hour. The grid was viewed under the TEM and images were taken. Further, samples were irradiated by 6.5 MeV electron beam for different fluences, varying from 5×10^{14} e/cm^2 to 4×10^{15} e/cm^2, using rack track microtron. Post irradiated nanophosphors were characterized by thermoluminescence technique (TL 1009I supplied by Nucleonix Systems Private Limited Hyderabad, India). The TL glow curves were recorded for 5 mg of sample each time by heating the samples at a uniform rate of 5 °C/s with the help of a temperature controller.

2.3 Conversion of dose in gray from the electron fluence

The dose D in the material by the electron energy deposition is calculated using the formula:

$$D = 1.602 \times 10^{-10} \times \frac{1}{\rho}\frac{dE}{dx} \times n \quad \ldots (2)$$

where the dose at the irradiated volume is expressed in Gy, the particle fluence, n is measured in cm^{-2}, ρ is the density of the irradiated material in g cm^{-3} and the main energy loss (dE/dx) is calculated using the

ESTAR code[18]. The doses for different electron fluences are shown in Table 1.

3 Results and Discussion

3.1 Crystal structure, particle size and TEM analysis

The XRD spectrum of nanocrytstalline $CaSO_4$: Eu phosphor is shown in Fig. 1. It reveals from Fig. 1 that the different peaks at (100), (110), (200), (102), (201), (211), (212) mainly exhibit hexagonal structure (JCPDS card No. 43-0606). The lattice parameters of the unit cell found to be a = 6.011 Å and c = 6.336 Å, respectively. The average particle (grain) size of the nanocrytstalline $CaSO_4$: Eu has been estimated from the line broadening of the XRD peaks. Assuming the particles are stress free, the size can be estimated from a single diffraction prominent peak using the Scherrer's formula:

$$d = \frac{0.9\,\lambda}{\beta\cos\theta} \qquad \ldots (3)$$

where d is the average grain size of the crystallites, λ is the incident wavelength, θ is the Bragg angle and β is the diffracted full width at half maximum (in radian) caused by the crystallites. The average grain size of the nanophosphor is estimated to be approximately around 15 nm, which confirms its nanocrystalline form. The shape and size of these nanoparticles have also been determined by the TEM. The TEM image as shown in Fig. 2 shows the nanorods having diameter 10-20 nm and length about 75-125 nm. It also shows that they are quite uniform in shapes and size. The selected area electron diffraction (SAED) pattern of nanophosphor shows crystalline nature of $CaSO_4$: Eu and confirms the hexagonal phase.

3.2 Thermoluminescence glow curves

Figure 3 shows the TL glow curves of $CaSO_4$: Eu nanophosphor irradiated at different fluences of 6.5 MeV energy electrons. TL spectra exhibit single glow peak at 173 °C and hump at 115 °C. The appearance of two peaks in the glow curve indicates that there are possibly two kinds of trapping sites due to electron irradiation, one at lower temperature and other at higher temperature. The first peak vanishes and the second peak shifts from 173 °C to 158 °C

Table 1 — Doses in gray from different electron fluences (e/cm^2) according to Eq. (2)

Electron fluence (e/cm^2)	Dose (kGy)
5×10^{14}	14.36
1×10^{15}	28.72
2×10^{15}	57.4
3×10^{15}	86.1
4×10^{15}	114.8

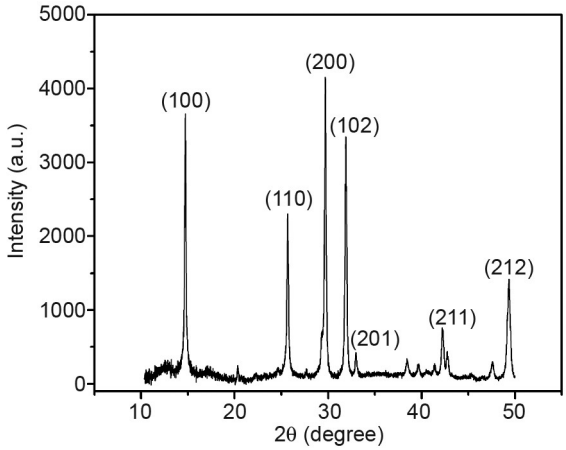

Fig. 1 — X-ray diffraction spectrum of a nanocrystalline $CaSO_4$: Eu phosphor

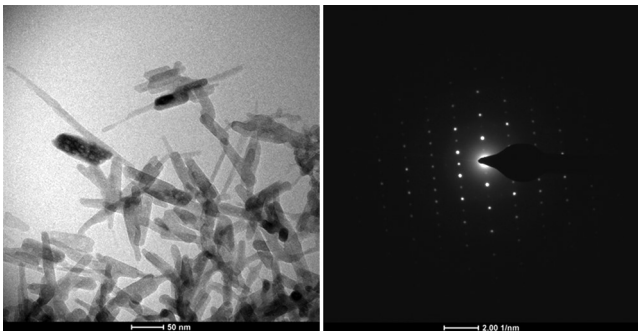

Fig. 2 — TEM and SAED pattern of $CaSO_4$: Eu nanophosphor

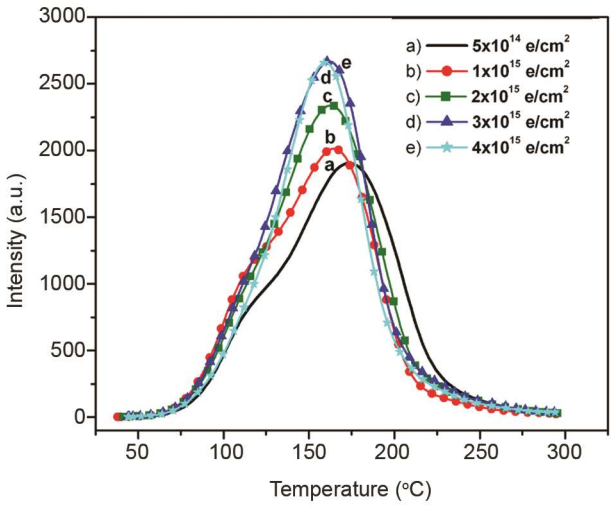

Fig. 3 — Thermoluminescence glow curves of $CaSO_4$: Eu nanophosphor irradiated at different 6.5 MeV energy electron fluences

with increase in the electron fluence from 5×10^{14} e/cm^2 to 4×10^{15} e/cm^2. This is mainly due to the disorganization of trapping centers (TCs)/luminescent centers[19] (LCs). The TL peak may be a first order, second order or general order of kinetics. In a second-order or general order reaction significant concentrations of released electrons are retrapped before they recombine, in this way giving rise to a delay in the luminescence emission and spreading out of the emission over a wider temperature range. If TL peak is a second order or general order then there is a shift in the peak. So the shift indicates that the peak is not a first order; it may be second or general order of kinetics[20,21]. For finding the order of kinetics and activation energy, deconvolution of glow curve is necessary. The peaks are deconvoluted and it is verified that the peaks are of general order as shown in Table 2.

3.3 Analysis of TL glow curves and calculation of trapping parameters by CGCD curve fitting by Kitis functions

The computerized glow curve deconvolution (CGCD) curve fitting was done using glow curve deconvolution (GCD) functions (Eqs (4) and (5)), suggested by Kitis[22], for general and first order kinetics glow curves, respectively. For kinetic analysis, the experimentally obtained TL glow curve was fitted with CGCD method[23].

For general order:

$$I(T) = I_m b^{\left(\frac{b}{b-1}\right)} \exp\left(\frac{E}{kT}\frac{T-T_m}{T_m}\right) \left[(b-1)\frac{T^2}{T_m^2}\left(1-\frac{2kT}{E}\right)\exp\left(\frac{E}{kT}\frac{T-T_m}{T_m}\right)+1+(b-1)\frac{2kT_m}{E}\right]^{-\frac{b}{b-1}} \quad \ldots (4)$$

For first order:

$$I(T) = I_m \exp\left[1+\frac{E}{kT}\frac{T-T_m}{T_m}-\frac{T^2}{T_m^2}\exp\left(\frac{E}{kT}\frac{T-T_m}{T_m}\right)\left(1-\frac{2kT}{E}\right)-\frac{2kT_m}{E}\right] \quad \ldots (5)$$

Here, $I(T)$ is the TL intensity at temperature T, I_m, the maximum peak intensity, T_m is the temperature corresponding to maximum peak intensity I_m, and E is trap depth or the thermal activation energy needed to free the trapped electrons, b is order of kinetics and k is the Boltzmann's constant (8.6×10^{-5} eVK^{-1}).

The frequency factor s is obtained from the following equations.

For general order:

$$s = \frac{\beta E}{kT_m^2\left(1+(b-1)\frac{2kT_m}{E}\right)}\exp\left(\frac{E}{kT_m}\right) \quad \ldots (6)$$

For first order:

$$s = \frac{\beta E}{kT_m^2}\exp\left(\frac{E}{kT_m}\right) \quad \ldots (7)$$

where β is the linear heating rate and b is the order of kinetics.

Figure 4 shows the de-convoluted TL curves and the theoretical curve fitting with the experimental TL curve for the sample irradiated with electron fluence of 3×10^{15} e/cm^2. The goodness of the fitting, i.e., figure of merit (FOM), is found to be 0.0238 (i.e., 2.38 %). This shows that experimental and theoretical glow curves are in good agreement and very much overlapping on either side. The residue curves of the

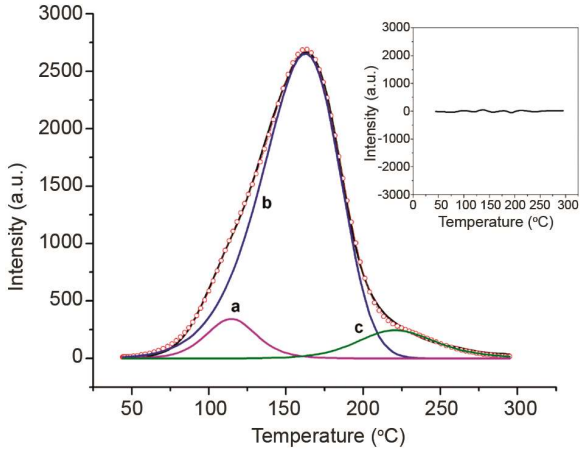

Fig. 4 — Comparison between the experimental (—) and the theoretically (○) fitted TL glow curves of $CaSO_4$: Eu nanophosphor powder exposed to electron fluence of 3×10^{15} e/cm^2. Curves a, b and c (—) are deconvoluted single fitted glow curves. Inset shows the residue curves for the experimental and theoretically fitted glow curves

Table 2 — Trapping parameters of $CaSO_4$: Eu nanophosphor for electron fluence of 3×10^{15}e/cm^2

Fluence (e/cm^2)	Peak	Peak temperature T_m (°C)	Peak temperature T_m (K)	Order of kinetics (b)	Trap Depth E (eV)	Frequency factor, s (s^{-1})	FOM %
	a	114	387	1.76	1.05	1.77×10^{13}	
3×10^{15}	*b*	162	435	1.085	0.65	6.70×10^{6}	2.38
	c	220	493	1.97	1.16	1.82×10^{11}	

theoretically fitted TL glow curves are also shown in the inset of Fig. 4. The deconvolution of the experimental curves has revealed some more glow peaks around 114 °C and 220 °C (curves a and c in Fig. 4) in addition to the obvious 162 °C peak (curve b in Fig. 4). The calculated trapping parameter has been given in Table 2.

To verify further, the activation energy (E) and order of kinetics (b) of the deconvoluted glow peaks of microcrystalline and nanocrystalline $CaSO_4$: Dy phosphor have been calculated using Chen's set of empirical formulae[24] as follows:

$$E_\alpha = c_\alpha \left(\frac{kT_m^2}{\alpha}\right) - b_\alpha(2kT_m) \quad \ldots (8)$$

with

$$\alpha = \tau, \delta, \omega,$$
$$\tau = T_m - T_1, \delta = T_2 - T_m, \omega = T_2 - T_1,$$
$$c_\tau = 1.51 + 3.0\left(\mu_g - 0.42\right),$$
$$c_\delta = 0.976 + 7.3\left(\mu_g - 0.42\right),$$
$$c_\omega = 2.52 + 10.2(\mu_g - 0.42),$$
$$b_\tau = 1.58 + 4.2(\mu_g - 0.42),$$
$$b_\delta = 0,$$
$$b_\omega = 1$$

To determine the order of kinetic, the form factor was calculated by using the equation:

$$\mu_g = \frac{T_2 - T_m}{T_2 - T_1} \quad \ldots (9)$$

Theoretically, the form factor μ_g ranges between 0.42 and 0.52, the value is close to 0.42 for first order kinetics and 0.52 for second order kinetics. To determine the general order of kinetics (other than first or second order), use of the correlation between order of kinetics (b) and the form factor (μ_g) given by Chen was made[25]. The average values of the activation energies calculated by Chen's set of equations very well matches with the values calculated by CGCD program using Kitis functions.

Trapping parameters of all the above peaks are summarized in Table 2. Peaks at 114 °C and 220 °C are close to second order peaks and peak at 162 °C is first order peak. It is obvious that a considerable amount of retrapping is taking place in 114 °C and 220 °C peaks, except the 162 °C peak (which is having first order of kinetics). The energy levels (activation energy) of various traps (corresponding to various peaks) are very much different. Therefore, it is clear that there are some deep and shallow traps and for this reason there could be retrapping of the electrons at deep traps while going to upper shallow traps by the stimulation due to heat energy. The competition among them might be giving various releasing and retrapping probabilities, which might have resulted in different frequency factors. The traps could be either electron traps or hole traps or of both kind. The order of kinetics is showing some alternate pattern from second to first order with the peaks appearing with increasing temperature, which shows that some hole traps are also involved more prominently in TL process[4].

3.4 TL response and fading

The TL response curve (peak heights with the electron dose) of $CaSO_4$: Eu nanophosphor irradiated with 6.5 MeV energy electrons is shown in Fig. 5. The peak heights are used for measuring TL intensity. It is observed from the figure that the TL peak intensity increases from 15 kGy to 80 kGy and further saturates beyond 80 kGy. The sublinear behavior of TL response curve can be explained on the basis of unified interaction model[26,27] (UNIM). The UNIM incorporates all the features of the track interaction model (TIM) for heavy charged particles and the defect interaction model for gamma rays and electrons in an identical conceptual and mathematical formalism. The major premise of the UNIM applied to the electron dose response is that the linear behavior arises due to a localized TC/LC entity which suppresses competitive processes for a certain fraction of the trapped charge carriers. In electron dose

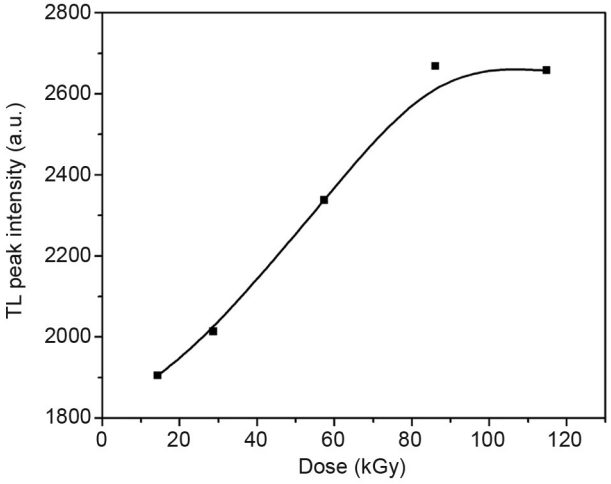

Fig. 5 — Variation in the TL peak intensity with electron dose for $CaSO_4$: Eu nanophosphor

response, especially at low dose, recombination occurs exclusively within the trapping entity (i.e., within TC/LC complex), leading to a linear dose response whereas at higher dose level the effectiveness of the non-radiative competing centers decreases. The competing centers are increasingly populated with increase in the dose and rendering them more and more ineffective, thereby leading to an increase in the luminescent efficiency. Further increase in dose a saturation effect occurs, where the distances between neighboring TC/LC complex decrease and the TC/LC complex begins to merge and overlap. The overlapping regions do not contribute to additional TL since they do not result in additional trapping charge carriers due to the full occupancy of the available trapping centers and luminescence centers.

Moreover, the linearity of the TL response for the nanophosphors over a wide range of dose may attribute to the high surface to volume ratio which results in a higher surface barrier energy for the nanorods[6]. The nanoparticles/nanorods have high surface barrier energy and 6.5 MeV energy of electron beam is high enough to cross this barrier. If electron fluence is increased, the surface barrier energy of the nanoparticles is crossed and large defects are produced in the nanophosphors. The number of defects created in the material keeps on increasing with electron fluence till saturation is obtained. But, in case of nanophosphor, saturation did not occur because of the existence of some particles that would have been missed while being targeted by the high energy radiation, due to their very tiny size. Thus, on increasing the electron fluence, these nanoparticles which had been left out from the interaction, now generate trapping centers (TCs)/luminescence centers (LCs). So, nanophosphors do not show saturation at higher doses. Thus, nanophosphor gives good linearity over a wide range of the doses. TL fading of $CaSO_4$: Eu nanophosphor was recorded and is also shown in Fig. 6. Around 8-10 % fading over 30 days was recorded for the 162 °C peak if irradiated with 3×10^{15} e/cm^2 electron fluence.

For dosimetric purposes, a thermoluminescent phosphor is expected to show the features such as it should have[13]: a relatively simple glow curve (no interfering glow peaks), high TL sensitivity, long term stability of the stored information at room temperature (namely low fading); good linearity of the TL signal in the specific useful range of radiation dose; effective atomic number, Z_{eff} close to that of the biological tissue (in order to deal with a tissue equivalent material). $CaSO_4$: Eu nanophosphor has a very good linear response over a wide range of dose from 15 kGy to 80 kGy considering these features of dosimetry. Moreover, it has a single major glow peak at 162 °C and has negligible fading (around 8-10%) over the period of 1 month. Therefore, this nanocrytstalline $CaSO_4$: Eu phosphor could be used for high dose measurement of electrons.

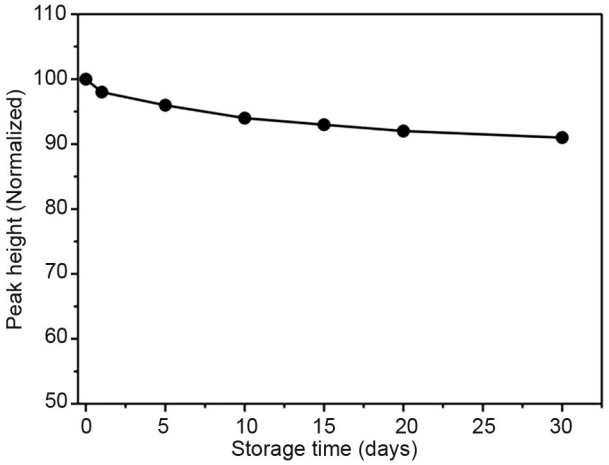

Fig. 6 — Fading curve for $CaSO_4$: Eu nanophosphor irradiated with 3×10^{15} e/cm^2 electron fluence

4 Conclusions

The $CaSO_4$: Eu nanophosphor exhibits hexagonal crystalline structure and diameter and length of the nanorods varied from 10-20 nm and 75 to 125 nm, respectively. The TL glow curve exhibits a single peak at 162 °C and a hump at 115 °C. TL glow curve is theoretically fitted using computerized glow curve deconvolution (CGCD) method and trapping parameters are calculated for different peaks. One peak is of first order and two peaks are of nearly second order. The activation energy of various peaks is very much different. Therefore, it is clear that there are some deep and shallow traps and for this reason there could be retrapping of the electrons at deep traps while going to upper shallow traps. The nanophosphor exhibited a sublinear TL response for the wide range of electron dose from 15 kGy to 80 kGy. The easy method of preparation, simple glow curve structure and better TL response are some of the good features of the $CaSO_4$: Eu nanophosphor. This phosphor can thus be effectively used for the measurement of high dose in space craft payload.

References

1 Gong X, Wu P, Chan W K & Chen W, *J Phys Chem Solids*, 61 (2000) 115.

2 Kasa I, Chobola R, Mell P, Szakacs S & Kerekes A, *Radiat Prot Dosim*, 123 (2007) 32.

3 Sahare P D & Moharil S V, *J Phys D: Appl Phys*, 23 (1990) 567.

4 Salah N, Sahare P D, Shah Nawaz & Lochab S P, *Radiat Effects Defects Solids*,159 (2004) 321.

5 Pandey A, Sonkawade R G & Sahare P D, *J Phys D: Appl Phys*, 35 (2002) 2744.

6 Pandey A, Bahl S, Sharma K, Ranjan R, Pratik Kumar & Lochab S P, *Nucl Instrum Meth B*, 269 (2011) 216.

7 Salah N, Sahare P D, Lochab S P & Kumar P, *Radiat Meas*, 41 (2006) 40.

8 Salah N, Sahare P D & Rupasov A A, *J Lumin*, 124 (2007) 357.

9 Lochab S P, Sahare P D, Chauhan R S, Salah N, Ranjan R & Pandey A, *J Phys D: Appl Phys*, 40 (2007) 1343.

10 Lochab S P, Kanjilal D, Salah N, Habib S S, Lochab J, Ranjan R, Aleynikov E, Rupasov A A & Pandey A, *J Appl Phys*, 104 (2008) 033520.

11 Shaila B, Pandey A, Lochab S P, Aleynikov V E, Molokanov A G & Kumar P, *J Lumin*, 134 (2013) 691.

12 Horowitz Y S & Moscovitch M, *Radiat Prot Dosim*, 153 (2013) 1.

13 Azorin J, Furetta C & Scacco A, *Phys Stat Sol A*, 138 (1993) 9.

14 Bapat V N, *J Phys C: Solid State Phys*, 10 (1977) L465.

15 Upadeo S V, Gundurao T K & Moharil S V, *J Phys: Condens Matter*, 6 (1994) 9459.

16 Upadeo S V & S V Moharil, *J Phys: Condens Matter*, 9 (1997) 735.

17 Nairy S R, Kondawary V K, Upadeoz S V, Moharil S V & Gundurao T K, *J Phys: Condens Matter*, 9 (1997) 8307.

18 Berger M J, Coursey J S, Zucker M A & Chang J, *Stopping-power and range tables for electrons, protons, and helium ions*, NIST, Physical Measurement Laboratory.

19 Gaikwad J, Thomas S, Kamble S, Vidyasagar P B & Sarma A, *Nucl Instrum Meth B*, 156 (1999) 231.

20 Bos A J J, *Radiat Meas*, 41 (2007) S45.

21 Bos A J J & Dielhof J B, *Radiat Prot Dosim*, 37 (4) (1991) 231.

22 Kitis G, Gomez-Ros J M & Tuyn J W N, *J Phys D*, 31 (1998) 2636.

23 Pagonis V, Kitis G & Furetta C, *Numerical and practical exercises in thermoluminescence*, (Springer Science-Business Media, Inc), 2006.

24 Chen R & Kirsh Y, *Analysis of thermally stimulated processes*, 1st Edn, (Pergamon Press, New York), 1981.

25 Chen R, *J Electrochem Soc*, 116 (1969) 1254.

26 Mahajna S & Horowitz Y S, *J Phys D: Appl Phys*, 30 (1997) 2603.

27 Horowitz Y S, *Nucl Instrum Meth B*, 184 (2001) 68.